Original Article

3D bone texture analysis as a potential predictor of radiation-induced insufficiency fractures

Valerio Nardone[1,2], Paolo Tini[1,2,3], Stefania Croci[1,2], Salvatore Francesco Carbone[4], Lucio Sebaste[1,2], Tommaso Carfagno[1,2], Giuseppe Battaglia[1,2], Pierpaolo Pastina[1,2], Giovanni Rubino[1,2], Maria Antonietta Mazzei[5], Luigi Pirtoli[1,2,6]

[1]Unit of Radiation Oncology, University Hospital of Siena, Siena, Italy; [2]Istituto Toscano Tumori, Florence, Italy; [3]Sbarro Health Research Organization, Temple University, Philadelphia, PA, USA; [4]Unit of Diagnostic Imaging, University Hospital of Siena, Siena, Italy; [5]Department of Medical, Surgical and Neuro Sciences, Diagnostic Imaging, University of Siena, Azienda Ospedaliera Universitaria Senese, Siena, Italy; [6]Department of Biology, College of Science and Technology, Temple University, Philadelphia, PA, USA

Correspondence to: Valerio Nardone, MD. Unit of Radiation Oncology, University Hospital of Siena, Viale Bracci, 53100 Siena, Italy.
Email: v.nardone@hotmail.it.

Background: The aim of our work is to assess the potential role of texture analysis (TA), applied to computed tomography (CT) simulation scans, in relation to the development of insufficiency fractures (IFs) in patients undergoing radiation therapy (RT) for pelvic malignancies.

Methods: We analyzed patients undergoing pelvic RT from Jan-2010 to Dec-2016, 31 of whom had developed IFs of the pelvis. We analyzed CT simulation scans using LifeX Software©, and in particular we selected three regions of interest (ROI): L5 body, the sacrum and both the femoral heads. The ROI were automatically contoured using the treatment planning software Raystation©. TA parameters included parameters from the gray-level histogram, indices from sphericity and from the matrix of GLCM (gray level co-occurrence matrix). The IFs patients were matched (1:1 ratio) with control patients who had not developed IFs, and were matched for age, sex, type of tumor, menopausal status, RT dose and use of chemotherapy. Univariate and multivariate analyses (logistic regression) were used for statistical analysis.

Results: Significant TA parameters on univariate analysis included both parameters from the histogram distribution, as well from the matrix of GLCM. On logistic regression analysis the significant parameters were L5-energy [P=0.033, odds ratio (OR): 1.997, 95% CI: 1.059–3.767] and FH-Skewness (P=0.014, OR: 2.338, 95% CI: 1.191–4.591), with a R2: 0.268. A ROC curve was generated from the binary logistic regression, and the AUC was 0.741 (95% CI: 0.627–0.855, P=0.001, S.E.: 0.058).

Conclusions: In our experience, 3D-bone CT TA can be used to stratify the risk of the patients to develop radiation-induced IFs. A prospective study will be conducted to validate these findings.

Keywords: Texture analysis (TA); side effects; insufficiency fractures (IFs); radiation therapy (RT)

Submitted Oct 16, 2017. Accepted for publication Feb 02, 2018.
doi: 10.21037/qims.2018.02.01
View this article at: http://dx.doi.org/10.21037/qims.2018.02.01

Introduction

Insufficiency fractures (IFs) are defined as a type of stress fracture, which can occur if a weakened bone, due to decreased elastic resistance and demineralization, is stressed with normal and/or physiological force.

Many pathological conditions are often associated with IFs, such as osteoporosis (1-4).

Recently, radiation therapy (RT) has been recognized as a risk factor for IFs (5) in many malignancies (6-10), ranging from 9% to 11.2% in rectal (11), 8.2% to 45.2% in cervical (12-14), and up to 6.8% (10) in prostate cancer, respectively. The risk factors for RT-induced IFs that have

been identified include post-menopausal state, older age, chemotherapy and female sex (8,11,13,14).

Texture analysis (TA) is able to quantify image heterogeneities that may not be appreciated with the naked eye, and represents a method based on mathematical analysis for the evaluation of gray-level intensity and for the position of the pixels within the images, providing "texture features", that represent a quantitative measure of various imaging techniques (15). Statistical analysis achieves and quantifies both distribution and relationships of the gray-level values of the image. Actually, many studies have considered TA in several areas of cancer imaging, showing a potential application in diagnosis, assessment of response to treatment as well as characterization of tumors (16-24). In regards of bone physiology, TA has been applied mainly for densitometry, leading to the development of the trabecular bone score (TBS), an analytical tool for gray-level texture measurements calculated on dual X-ray absorptiometry (DXA) of the lumbar spine, thus providing information related to trabecular architecture (25-27).

We have previously studied the efficacy of bone TA, using a home-made ImageJ macro and selecting only two 2D ROI (the vertebral body of L5 and the femoral head) in a case-control study (28,29).

With these premises, we have investigated in the present study the potential role of TA based on 3D ROI, automatically contoured using the treatment planning software Raystation©. TA parameters were calculated using LifeX Software© (30), and included parameters from the gray-level histogram and from the matrix of GLCM (gray level co-occurrence matrix).

Methods

Patients

IF cohort of patients (IF-p)

From January 2009 to December 2016, 31 patients that were previously treated for pelvic malignancies developed pelvic IFs during the follow-up. We collected all the clinical data, as well as the pathological and dosimetric information, for the present study.

The IF-p series included 14 patients (46%) with endometrial or cervical cancer, 15 patients (48%) with anal or rectal cancer and 2 (6%) with prostate or bladder tumors.

A CT simulation for treatment planning calculations was done before RT. Previous fractures of the pelvic bone and any tumor recurrence were considered as a cause of exclusion.

In this regard, we have excluded twelve patients from this analysis (five patients showed evidence of IFs before the radiation treatment and seven patients developed bone tumor recurrence).

Controlled patients cohort (C-p)

The IF-p patients were compared (1:1 ratio) with the C-p series, which were similarly patients submitted to pelvic irradiation in our institution in the same time-lapse, but not developing IFs. Each IF-p patient was matched with one C-p patient, for the criteria of sex, menopausal status, age, localization of tumor, chemotherapy and RT dose. The exclusion criteria were identical.

In order to limit biases, we also considered the time-lapse of RT administration (Jan 2009 to Dec 2012 *vs.* Jan 2013 to Dec 2016), the RT total doses and the RT technique [intensity-modulated RT (IMRT) *vs.* three-dimensional conformal RT (3D-CRT)].

Radiotherapy and chemotherapy treatment

RT was given with a Linear Accelerator, with 6 or 15 MeV photon beams. 3D-CRT or IMRT techniques were chosen according to the clinician choice. Target volumes and organs at risk were identified by diagnostic CT and contoured on simulation CT.

Chemotherapy was administered concurrently with, or sequentially to, RT, employing standard association of platinum, fluoropyrimidine compounds, mitomycin and taxanes, according to international guidelines.

Specifically, patients with cervical cancer underwent chemotherapy with weekly cisplatin (40 mg/m^2), patients with rectal cancer underwent chemotherapy with capecitabine (825 mg/m^2, twice daily for 5 days/week) daily throughout the radiotherapy course, and patients with anal canal cancer underwent chemotherapy with 5-FU (1,000 mg/m^2/day) by continuous infusion for 4 days and MMC (10 mg/m^2) intravenous bolus for two cycles during the course of RT.

Authorization for the retrospective analysis was given by the Internal Institutional Review Board.

Each patient signed an informed consent both for the treatments and for the anonymous use of clinical data. All procedures were in compliance with the ethical statements of the Helsinki Declaration (1964, amended most recently in 2008).

Follow-up

After completion of treatment, all patients underwent scheduled follow-up visits, according to the primary tumor. In patients with gynecological, gastrointestinal and bladder malignancies, an imaging with CT and/or MRI was performed at 4–6 and 12–16 weeks after the completion of RT, then every 6 months. In patients with prostate cancer, diagnostic CT and/or MRI was obtained only if justified by a rise of the PSA value and/or by emerging symptoms or physical signs of recurrence or complications.

The MRI examination was obtained with a 1.5-T system, Signa Excite HD, GE Healthcare, Milwaukee, WI, USA, whereas the CT was performed with a 64-detector row CT scanner (Discovery 750 HD, GE Healthcare, Milwaukee, WI, USA).

All the patients underwent a physical examination, chemistry and blood counts every 3 months.

Assessment of IFs

IFs development was confirmed at CT or MR imaging, by an expert radiologist (Salvatore Francesco Carbone), with 15 years' experience in the oncologic field. CT findings of IF included sclerotic linear changes or fracture lines, whereas MRI findings included both on T1 and T2-weighted images the presence of signal intensity changes in the bones of >5 mm (8).

In all the patients with IFs the simulation CT scan was reviewed, in order to exclude the patients that showed pre-existent fractures.

CT simulation

CT simulation was performed before RT, with a 16 slice CT-scanner (slice thickness 2.5 mm, beam pitch of 1.375, reconstruction interval 2.5 mm, tube voltage of 120 kVp and reference mAs ranging from 100 to 440 mA, Index Noise 10).

Image analysis

We analyzed three regions of interest (ROI) on CT simulation: the vertebral body of L5, the sacrum (S1–S3) and the femoral heads (*Figure 1*). Each ROI was automatically contoured using a treatment planning contouring workstation (RayStation©) and validated by a radiation oncologist (Valerio Nardone).

The TA was performed using a LifeX© (30), and included features of gray-level co-occurrence matrix (GLCM), sphericity and indices from the gray-level histogram. For the femoral heads ROI we calculated the mean of the two ROI.

Statistics

The TA parameters, as described above, were correlated with the development of IFs by univariate (Pearson correlation). We analyzed the correlation between the significant TA parameters and, if a correlation larger than 0.80 was observed, then the variable with the lowest univariable correlation with the endpoint was omitted, to avoid the risk of overfitting the model and of multicollinearity (31) in the multivariate analysis (binary logistic regression). After performing the multivariate analysis the ROC Curves with these parameters were also carried out. The statistical analysis was performed using the SPSS software 23.0.

Results

The characteristics of both the cohorts of IF-p and C-p, with the localizations of the IFs are reported in *Table 1*. IFs occurred in different pelvic bones, with 17 patients (55%) developed multiple IFs.

The median follow-up period was equal to 43.46 months (mean 47.21 months, SD 24.26 months, range 12–84 months).

Regarding the enrollment time-lapse, 15 out of 31 patients (48%) in IF-p series and 16 out of 31 patients (52%) in C-p series were enrolled from Jan 2009 to Dec 2012, whereas 16 out of 31 patients (52%) in IF-p series and 15 out of 31 patients (48%) in C-p series were enrolled from Jan 2013 to Dec 2016 (P>0.05). Regarding the RT technique 16 out of 31 patients (52%) in IF-p series and 17 out of 31 patients (55%) in C-p series underwent intensity modulated radiation therapy (IMRT), whereas 15 out of 31 patients (48%) in IF-p series and 14 out of 31 patients (45%) in C-p series underwent 3D-conformal RT, 3D-CRT (P>0.05). The period of enrollment, as well as the radiation doses between IF-p and C-p were well balanced between the groups (see the results reported in *Table 1*).

Univariate analysis

We performed a Pearson correlation analysis between the TA parameters and the development of IFs.

Significant TA parameters included: L5-kurtosis (P=0.049),

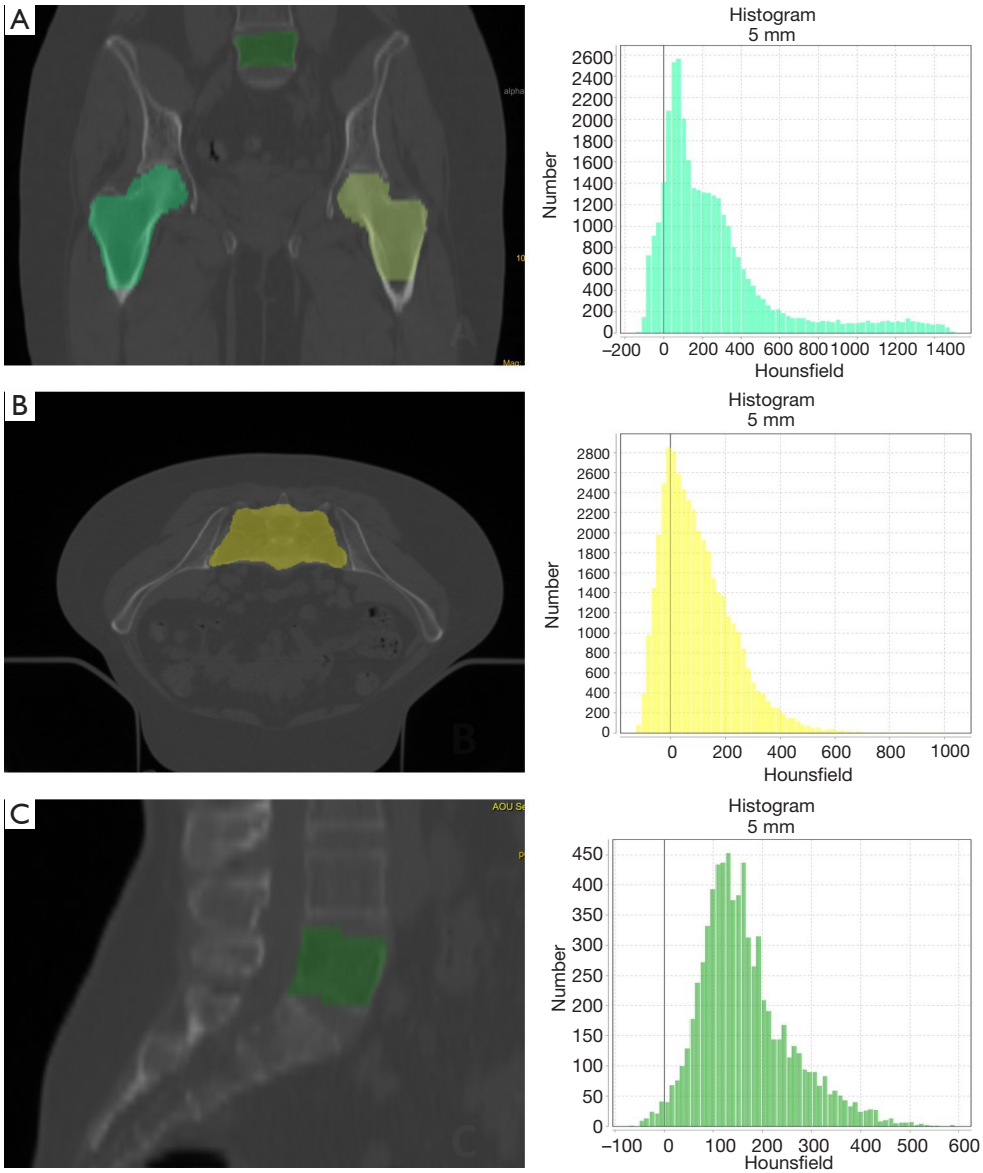

Figure 1 Examples of ROI and histograms of the pixel distribution (CT simulation DICOM images): (A) femoral head ROI; (B) sacrum ROI; (C) L5 ROI. ROI, regions of interest; DICOM, Digital Imaging and Communications in Medicine.

L5-energy (P=0.007), L5-GLCM-energy (P=0.023), sacrum-kurtosis (P=0.034), sacrum-compacity (P=0.039, this parameters is a measure of compactness of the volume), FH-kurtosis (P=0.005), FH-skewness (P=0.001), FH-energy (P=0.005), FH-GLCM-homogeneity (P=0.006), FH-GLCM-energy (P=0.020) (*Tables 2,3* and *Figure 2*).

Multivariate analysis

The TA parameters that resulted significantly at univariate analysis were normalized and tested for co-correlation. The parameters L5-GLCM-energy, FH-kurtosis, FH-energy were omitted, to avoid the risk of overfitting the model and of multicollinearity (31) in the multivariate analysis.

We performed a logistic regression analysis with the group as the dependent variable and all the normalized texture parameters, plus all relevant confounding variables (sex, radiation doses, and chemotherapy).

The variables that resulted significant were L5-energy [P=0.033, odds ratio (OR): 1.997, 95% CI: 1.059–3.767] and

Table 1 Characteristics of patients in the insufficiency fracture (IF-p) and control (C-p) series

Characteristics of patients	IF-p series	C-p series
Sex		
Male	9 (29%)	9 (29%)
Female	22 (71%)	22 (71%)
Age: mean (range)	65.7±10.21 (range, 30–81) years	64.9±11.24 (range, 32–80) years
Menopausal status		
Pre-menopausal	8 (36%)	7 (32%)
Post-menopausal	14 (64%)	15 (68%)
Disease		
Gynecological	14 (46%)	14 (46%)
Gastrointestinal	15 (48%)	15 (48%)
Urological	2 (6%)	2 (6%)
Chemotherapy	Yes: 19 (61%)	Yes: 19 (61%)
	No: 12 (39%)	No: 12 (39%)
RT target dose (PTV): mean (range)	5,030±510 (range, 4,500–5,940) cGy	5,050±540 (range, 4,500–5,940) cGy
Localization of the IFs		
Sacroiliac joints	18 (58%)	
Pubis	7 (23%)	
Acetabulum	4 (13%)	
Sacral body	7 (23%)	
Lumbar vertebrae	6 (19%)	
RT technique		
IMRT	16/31 (52%)	17/31 (55%)
3D/CRT	15/31 (48%)	14/31 (45%)
Enrollment period		
Jan 2009 to Dec 2012	15/31 (48%)	16/31 (52%)
Jan 2013 to Dec 2016	16/31 (52%)	15/31 (48%)

FH-skewness (P=0.014, OR: 2.338, 95% CI: 1.191–4.591), with a R^2: 0.268 (*Tables 2,3*).

A ROC curve was generated from the binary logistic regression, the AUC was 0.741 (95% CI: 0.627–0.855, P=0.001, S.E.: 0.058) (*Figure 3*).

Discussion

We have previously studied (28,29) the role of bone TA, with an in-house 2D software, and we have decided to explore the potential role of 3D Bone TA. Moreover, we tested the possibility of automatically obtain 3D ROI with the treatment planning contouring workstation (Raystation©).

Although the LifeX Software© (30) is able to calculate parameters of gray-level co-occurrence matrix (GLCM), neighbourhood gray-level dependence matrix (NGLDM), gray-level run length matrix (GLRLM), gray-level zone length matrix (GLZLM), sphericity and indices from the gray-level histogram, we decided to use only parameters

Table 2 Pearson univariate analysis

TA parameters	IF-p series (mean ± SD)	C-p series (mean ± SD)	P value
Kurtosis (L5)	5.98±1.92	5.23±1.23	0.049
Energy (L5)	0.050±0.0098	0.044±0.006	0.007
GLCM-energy (L5)	0.0049±0.0018	0.0041±0.0011	0.023
Kurtosis (sacrum)	6.791±2.42	5.78±1.50	0.034
Compacity (sacrum)	3.86±1.26	3.40±0.50	0.039
Kurtosis (FH)	6.58±1.60	5.73±0.85	0.005
Skewness (FH)	1.86±0.25	1.68±0.19	0.001
Energy (FH)	0.041±0.0059	0.038±0.0041	0.005
GLCM-homogeneity (FH)	0.38±0.026	0.37±0.020	0.006
GLCM-energy (FH)	0.0046±0.0013	0.0040±0.00098	0.020

TA, texture analysis; GLCM, gray-level co-occurrence matrix; IF, insufficiency fracture; FH, femoral head.

Table 3 Binary logistic regression analysis (normalized odds ratio)

Parameter	P value	Odds ratio	95% CI
Energy (L5)	0.033	1.997	1.059–3.767
Skewness (FH)	0.014	2.338	1.191–4.591

FH, femoral head.

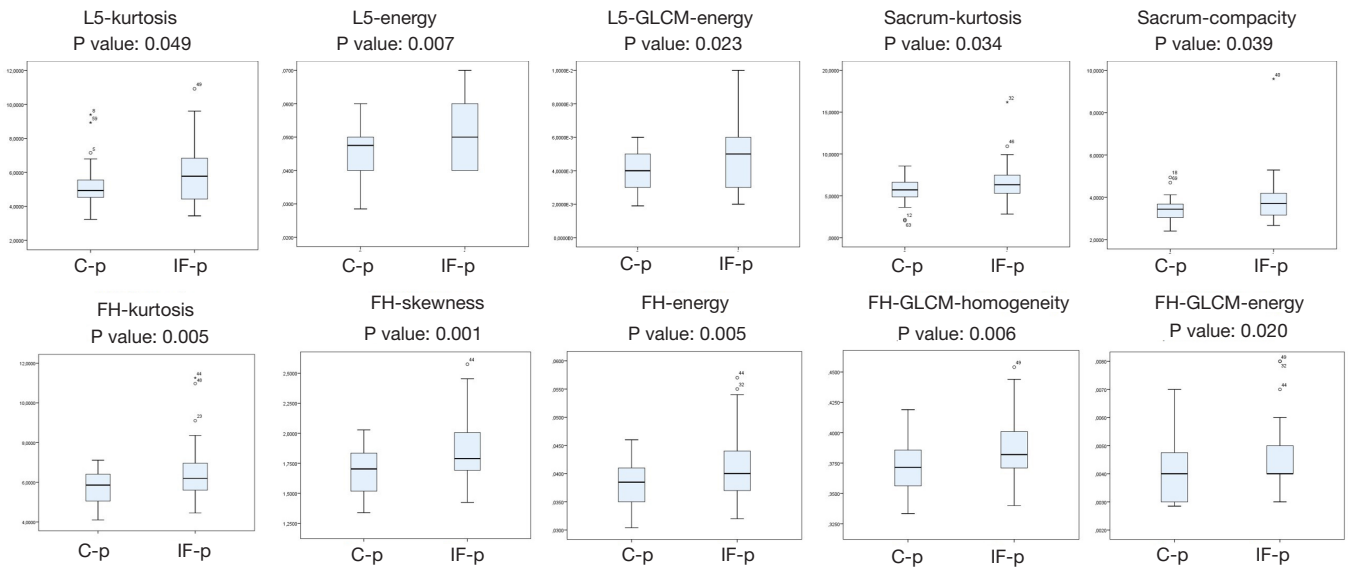

Figure 2 Box Plot in IF-p and C-p patients (univariate analysis). IF, insufficiency fracture. IF-p, insufficiency fracture cohort of patients; C-p, controlled patients cohort.

from gray-level histogram, sphericity and GLCM matrix, to reduce the number of TA variables, including TA indices that were already used in the imaging of trabecular bone structure (32).

At this regard, the major novelties of this paper, in comparison to our previous work (28), are the 3D TA, the automatic contouring of the ROI and the higher number of texture parameters analysed.

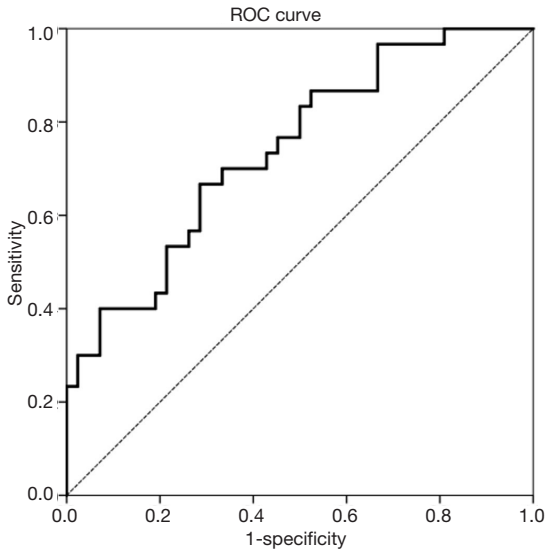

Figure 3 ROC curve generated from binary logistic regression. AUC 0.741 (95% CI: 0.627–0.855, P=0.001, S.E.: 0.058). ROC, receiver operating characteristic curve; AUC, area under the curve.

Our results showed a co-correlation between many variables, as well as the significance of the same TA variables between the different ROI (energy, kurtosis), and this aspect increases the validity of our results.

The TA variables that resulted significant at binary logistic regression were L5-energy and FH-skewness.

Energy represents a measure of the uniformity of the distribution, and is significantly higher in IF-p than C-p. This parameter is inversely correlated to the entropy, in accordance with previous works (28,33,34). This might be explained by the fibers being more marked in the control group, with an increase in the randomness of the pixel values, and eventually an increase in the entropy and a decrease in energy.

Skewness, on the other hand, measures the asymmetry of the gray-level distribution in the histogram, and this parameter was higher in IF-p than C-p. This result could be correlated to a lower density (35) and mineralization of the bone, thus reflecting a higher asymmetry in the histogram.

We have summarized the various studies of bone TA in *Table 4*.

However, the interpretation of TA parameters on the grounds of bone pathophysiology is incomplete, thus our study is still awaiting an exhaustive scientific background.

In fact, radiation-induced bone damage has been

Table 4 Comparison of different studies regarding bone texture analysis

References	Texture parameters	Findings
Current work	L5-energy	Measure of the uniformity of the distribution, and is higher in patients developing IFs
	FH-skewness	Measure of the asymmetry of the gray-level distribution in the histogram, and is higher in patients developing IFs
Nardone *et al.* (28)	L5—entropy and uniformity	Entropy was lower in IFs, and uniformity was higher
	FH—mean and standard deviation CT	Mean and standard deviation were significantly lower in the IF-p
Uezono *et al.* (35)	CT density of bone and bone marrow	Lower density of bone and bone marrow in the IF-p
Harvey *et al.* (25)	TBS, a measure of grey-level texture measurements on lumbar spine dual X-ray absorptiometry (DXA) images	Measure of trabecular microarchitecture, is lower in patients developing IFs
Rachidi *et al.* (33)	Mean, standard deviation and entropy	All these parameters were significantly lower in patients developing IFs
Thevenot *et al.* (34)	Entropy	Entropy was lower in IF-patients

IF, insufficiency fracture.

described since the early years of the twentieth century, but the pathophysiology is still unclear. Irradiation seems to reduce osteoblast number, arrest osteoblast cell cycle progression and promote apoptosis, leading to a reduced bone formation (36-38). Data for osteoclasts effect are in some way contradictory (39,40), whereas the damages on bone matrix and on the vascular supply are established (41,42). The combination of these effects results in a reduction in the bone mineral density (BMD) in patients undergoing pelvic RT (43).

The incidence of IF seems to be higher than expected, although there are many discrepancies in the various study (5,10-14,44-46), probably due to the differences in the follow-up, as the choice of imaging may increase the detection of asymptomatic IFs. One study reported 89% of patients had findings compatible with IF after pelvic RT using magnetic resonance imaging (47), while another study reported 34% using bone scintigraphy (48).

It is noteworthy that currently there is no recommendation for the diagnosis and the management of radiation-related IF in patients undergoing pelvic radiotherapy.

Very recently (25-27), the TBS measurement of gray level texture on DXA images has provided some information on microarchitecture of the trabecular bone, and these parameters seem associated with an increase in both prevalent and incident fractures. These information, also, seem to be independent from the clinical risk factors and BMD.

Limitations of the study

Although our method of TA has improved with the use of automatically contoured ROI, 3D TA and a higher number of TA parameters, our results still need methodological and technical refinements, as wells as a validation in larger series and prospective trials.

The low number of patients enrolled, as well as the matched analysis comparison, also represent a limit of our study.

Conclusions

Insufficiency fractures represent an important cause of morbidity for cancer survivors undergone pelvic radiotherapy and there is a need to develop robust clinical interventions that are evidence-based.

Our results appear to be promising since the knowledge of the predictive factors of this kind of RT toxicity could drive the selection of the best appropriate preventions in the population at risk.

We're planning to start a prospective trial, integrating bone mineralometry and serum markers, to further substantiate this field of investigation.

Acknowledgements

None.

Footnote

Conflicts of Interest: The authors have no conflicts of interest to declare.

Ethical Statement: Authorization for the retrospective analysis was given by the Internal Institutional Review Board. Each patient signed an informed consent both for the treatments and for the anonymous use of clinical data. All procedures were in compliance with the ethical statements of the Helsinki Declaration (1964, amended most recently in 2008).

References

1. Pacheco R, Stock H. Effects of radiation on bone. Curr Osteoporos Rep 2013;11:299-304.
2. Pentecost RL, Murray RA, Brindley HH. Fatigue, Insufficiency, and Pathologic Fractures. JAMA 1964;187:1001-4.
3. Peh WC, Gough AK, Sheeran T, Evans NS, Emery P. Pelvic insufficiency fractures in rheumatoid arthritis. Br J Rheumatol 1993;32:319-24.
4. Finiels H, Finiels PJ, Jacquot JM, Strubel D. Fractures of the sacrum caused by bone insufficiency. Meta-analysis of 508 cases. Presse Med 1997;26:1568-73.
5. Baxter NN, Habermann EB, Tepper JE, Durham SB, Virnig BA. Risk of pelvic fractures in older women following pelvic irradiation. JAMA 2005;294:2587-93.
6. Huh SJ, Kim B, Kang MK, Lee JE, Lim DH, Park W, Shin SS, Ahn YC. Pelvic insufficiency fracture after pelvic irradiation in uterine cervix cancer. Gynecol Oncol 2002;86:264-8.
7. Shih KK, Folkert MR, Kollmeier MA, Abu-Rustum NR, Sonoda Y, Leitao MM Jr, Barakat RR, Alektiar KM. Pelvic insufficiency fractures in patients with cervical and endometrial cancer treated with postoperative pelvic radiation. Gynecol Oncol 2013;128:540-3.

8. Tokumaru S, Toita T, Oguchi M, Ohno T, Kato S, Niibe Y, Kazumoto T, Kodaira T, Kataoka M, Shikama N, Kenjo M, Yamauchi C, Suzuki O, Sakurai H, Teshima T, Kagami Y, Nakano T, Hiraoka M, Mitsuhashi N, Kudo S. Insufficiency fractures after pelvic radiation therapy for uterine cervical cancer: an analysis of subjects in a prospective multi-institutional trial, and cooperative study of the Japan Radiation Oncology Group (JAROG) and Japanese Radiation Oncology Study Group (JROSG). Int J Radiat Oncol Biol Phys 2012;84:e195-200.
9. Allal AS, Mermillod B, Roth AD, Marti MC, Kurtz JM. Impact of clinical and therapeutic factors on major late complications after radiotherapy with or without concomitant chemotherapy for anal carcinoma. Int J Radiat Oncol Biol Phys 1997;39:1099-105.
10. Igdem S, Alco G, Ercan T, Barlan M, Ganiyusufoglu K, Unalan B, Turkan S, Okkan S. Insufficiency fractures after pelvic radiotherapy in patients with prostate cancer. Int J Radiat Oncol Biol Phys 2010;77:818-23.
11. Kim HJ, Boland PJ, Meredith DS, Lis E, Zhang Z, Shi W, Yamada YJ, Goodman KA. Fractures of the sacrum after chemoradiation for rectal carcinoma: incidence, risk factors, and radiographic evaluation. Int J Radiat Oncol Biol Phys 2012;84:694-9.
12. Ogino I, Okamoto N, Ono Y, Kitamura T, Nakayama H. Pelvic insufficiency fractures in postmenopausal woman with advanced cervical cancer treated by radiotherapy. Radiother Oncol 2003;68:61-7.
13. Ikushima H, Osaki K, Furutani S, Yamashita K, Kishida Y, Kudoh T, Nishitani H. Pelvic bone complications following radiation therapy of gynecologic malignancies: clinical evaluation of radiation-induced pelvic insufficiency fractures. Gynecol Oncol 2006;103:1100-4.
14. Oh D, Huh SJ, Nam H, Park W, Han Y, Lim do H, Ahn YC, Lee JW, Kim BG, Bae DS, Lee JH. Pelvic insufficiency fracture after pelvic radiotherapy for cervical cancer: analysis of risk factors. Int J Radiat Oncol Biol Phys 2008;70:1183-8.
15. Kato H, Kanematsu M, Zhang X, Saio M, Kondo H, Goshima S, Fujita H. Computer-aided diagnosis of hepatic fibrosis: preliminary evaluation of MRI texture analysis using the finite difference method and an artificial neural network. AJR Am J Roentgenol 2007;189:117-22.
16. Ganeshan B, Skogen K, Pressney I, Coutroubis D, Miles K. Tumour heterogeneity in oesophageal cancer assessed by CT texture analysis: preliminary evidence of an association with tumour metabolism, stage, and survival. Clin Radiol 2012;67:157-64.
17. Huang YL, Chen JH, Shen WC. Diagnosis of hepatic tumors with texture analysis in nonenhanced computed tomography images. Acad Radiol 2006;13:713-20.
18. Nardone V, Tini P, Biondi M, Sebaste L, Vanzi E, De Otto G, Rubino G, Carfagno T, Battaglia G, Pastina P, Cerase A, Mazzoni LN, Banci Buonamici F, Pirtoli L. Prognostic Value of MR Imaging Texture Analysis in Brain Non-Small Cell Lung Cancer Oligo-Metastases Undergoing Stereotactic Irradiation. Cureus 2016;8:e584.
19. Nardone V, Tini P, Nioche C, Biondi M, Sebaste L, Mazzei MA, Banci Buonamici F, Pirtoli L. Texture analysis of parotid gland as a predictive factor of radiation induced xerostomia: A subset analysis. Radiother Oncol 2017;122:321.
20. Nardone V, Tini P, Nioche C, Mazzei MA, Carfagno T, Battaglia G, Pastina P, Grassi R, Sebaste L, Pirtoli L. Texture analysis as a predictor of radiation-induced xerostomia in head and neck patients undergoing IMRT. Radiol Med 2018. [Epub ahead of print]. doi: 10.1007/s11547-017-0850-7.
21. Giganti F, Marra P, Ambrosi A, Salerno A, Antunes S, Chiari D, Orsenigo E, Esposito A, Mazza E, Albarello L, Nicoletti R, Staudacher C, Del Maschio A, De Cobelli F. Pre-treatment MDCT-based texture analysis for therapy response prediction in gastric cancer: Comparison with tumour regression grade at final histology. Eur J Radiol 2017;90:129-37.
22. Giganti F, Antunes S, Salerno A, Ambrosi A, Marra P, Nicoletti R, Orsenigo E, Chiari D, Albarello L, Staudacher C, Esposito A, Del Maschio A, De Cobelli F. Gastric cancer: texture analysis from multidetector computed tomography as a potential preoperative prognostic biomarker. Eur Radiol 2017;27:1831-9.
23. Narang S, Kim D, Aithala S, Heimberger AB, Ahmed S, Rao D, Rao G, Rao A. Tumor image-derived texture features are associated with CD3 T-cell infiltration status in glioblastoma. Oncotarget 2017;8:101244-54.
24. Chee CG, Kim YH, Lee KH, Lee YJ, Park JH, Lee HS, Ahn S, Kim B. CT texture analysis in patients with locally advanced rectal cancer treated with neoadjuvant chemoradiotherapy: A potential imaging biomarker for treatment response and prognosis. PLoS One 2017;12:e0182883.
25. Harvey NC, Gluer CC, Binkley N, McCloskey EV, Brandi

ML, Cooper C, Kendler D, Lamy O, Laslop A, Camargos BM, Reginster JY, Rizzoli R, Kanis JA. Trabecular bone score (TBS) as a new complementary approach for osteoporosis evaluation in clinical practice. Bone 2015;78:216-24.
26. Bousson V, Bergot C, Sutter B, Thomas T, Bendavid S, Benhamou CL, Blain H, Brazier M, Breuil V, Briot K, Chapurlat R, Chapuis L, Cohen Solal M, Fardellone P, Feron JM, Gauvain JB, Laroche M, Legrand E, Lespessailles E, Linglart A, Marcelli C, Roux C, Souberbielle JC, Tremollieres F, Weryha G, Cortet B, Groupe de Recherche et d'Information sur les O. Trabecular Bone Score: Where are we now? Joint Bone Spine 2015;82:320-5.
27. Di Gregorio S, Del Rio L, Rodriguez-Tolra J, Bonel E, Garcia M, Winzenrieth R. Comparison between different bone treatments on areal bone mineral density (aBMD) and bone microarchitectural texture as assessed by the trabecular bone score (TBS). Bone 2015;75:138-43.
28. Nardone V, Tini P, Carbone SF, Grassi A, Biondi M, Sebaste L, Carfagno T, Vanzi E, De Otto G, Battaglia G, Rubino G, Pastina P, Belmonte G, Mazzoni LN, Banci Buonamici F, Mazzei MA, Pirtoli L. Bone texture analysis using CT-simulation scans to individuate risk parameters for radiation-induced insufficiency fractures. Osteoporos Int 2017;28:1915-23.
29. Nardone V, Tini P, Sebaste L, Biondi M, Banci Buonamici F, Pirtoli L. Bone structure texture analysis as a potential tool to estimate radiation induced insufficiency fracture risk. Radiother Oncol 2016;120:184.
30. Nioche C, Orlhac F, Boughdad S, Reuze S, Soussan M, Robert C, Barakat C, Buvat I. A freeware for tumor heterogeneity characterization in PET, SPECT, CT, MRI and US to accelerate advances in radiomics. J Nucl Med 2017;58:Abstrat 1316.
31. van der Schaaf A, Xu CJ, van Luijk P, Van't Veld AA, Langendijk JA, Schilstra C. Multivariate modeling of complications with data driven variable selection: guarding against overfitting and effects of data set size. Radiother Oncol 2012;105:115-21.
32. Shirvaikar M, Huang N, Dong XN. The Measurement of Bone Quality Using Gray Level Co-Occurrence Matrix Textural Features. J Med Imaging Health Inform 2016;6:1357-62.
33. Rachidi M, Marchadier A, Gadois C, Lespessailles E, Chappard C, Benhamou CL. Laws' masks descriptors applied to bone texture analysis: an innovative and discriminant tool in osteoporosis. Skeletal Radiol 2008;37:541-8.
34. Thevenot J, Hirvasniemi J, Pulkkinen P, Maatta M, Korpelainen R, Saarakkala S, Jamsa T. Assessment of risk of femoral neck fracture with radiographic texture parameters: a retrospective study. Radiology 2014;272:184-91.
35. Uezono H, Tsujino K, Moriki K, Nagano F, Ota Y, Sasaki R, Soejima T. Pelvic insufficiency fracture after definitive radiotherapy for uterine cervical cancer: retrospective analysis of risk factors. J Radiat Res 2013;54:1102-9.
36. Sakurai T, Sawada Y, Yoshimoto M, Kawai M, Miyakoshi J. Radiation-induced reduction of osteoblast differentiation in C2C12 cells. J Radiat Res 2007;48:515-21.
37. Gal TJ, Munoz-Antonia T, Muro-Cacho CA, Klotch DW. Radiation effects on osteoblasts in vitro: a potential role in osteoradionecrosis. Arch Otolaryngol Head Neck Surg 2000;126:1124-8.
38. Szymczyk KH, Shapiro IM, Adams CS. Ionizing radiation sensitizes bone cells to apoptosis. Bone 2004;34:148-56.
39. Sawajiri M, Mizoe J, Tanimoto K. Changes in osteoclasts after irradiation with carbon ion particles. Radiat Environ Biophys 2003;42:219-23.
40. Willey JS, Lloyd SA, Robbins ME, Bourland JD, Smith-Sielicki H, Bowman LC, Norrdin RW, Bateman TA. Early increase in osteoclast number in mice after whole-body irradiation with 2 Gy X rays. Radiat Res 2008;170:388-92.
41. Green DE, Adler BJ, Chan ME, Lennon JJ, Acerbo AS, Miller LM, Rubin CT. Altered composition of bone as triggered by irradiation facilitates the rapid erosion of the matrix by both cellular and physicochemical processes. PLoS One 2013;8:e64952.
42. Scheller EL, Rosen CJ. What's the matter with MAT? Marrow adipose tissue, metabolism, and skeletal health. Ann N Y Acad Sci 2014;1311:14-30.
43. Hui SK, Khalil A, Zhang Y, Coghill K, Le C, Dusenbery K, Froelich J, Yee D, Downs L. Longitudinal assessment of bone loss from diagnostic computed tomography scans in gynecologic cancer patients treated with chemotherapy and radiation. Am J Obstet Gynecol 2010;203:353.e1-7.
44. Kwon JW, Huh SJ, Yoon YC, Choi SH, Jung JY, Oh D, Choe BK. Pelvic bone complications after radiation therapy of uterine cervical cancer: evaluation with MRI. AJR Am J Roentgenol 2008;191:987-94.
45. Reginelli A, Silvestro G, Fontanella G, Sangiovanni A, Conte M, Nuzzo I, Calvanese M, Traettino M, Ferraioli P, Grassi R, Manzo R, Cappabianca S. Validation of DWI in assessment of radiotreated bone metastases in elderly

patients. Int J Surg 2016;33 Suppl 1:S148-53.
46. Arrigoni F, Bruno F, Zugaro L, Natella R, Cappabianca S, Russo U, Papapietro VR, Splendiani A, Di Cesare E, Masciocchi C, Barile A. Developments in the management of bone metastases with interventional radiology. Acta Biomed 2018;89:166-74.
47. Blomlie V, Rofstad EK, Talle K, Sundfor K, Winderen M, Lien HH. Incidence of radiation-induced insufficiency fractures of the female pelvis: evaluation with MR imaging. AJR Am J Roentgenol 1996;167:1205-10.
48. Abe H, Nakamura M, Takahashi S, Maruoka S, Ogawa Y, Sakamoto K. Radiation-induced insufficiency fractures of the pelvis: evaluation with 99mTc-methylene diphosphonate scintigraphy. AJR Am J Roentgenol 1992;158:599-602.

Cite this article as: Nardone V, Tini P, Croci S, Carbone SF, Sebaste L, Carfagno T, Battaglia G, Pastina P, Rubino G, Mazzei MA, Pirtoli L. 3D bone texture analysis as a potential predictor of radiation-induced insufficiency fractures. Quant Imaging Med Surg 2018;8(1):14-24. doi: 10.21037/qims.2018.02.01

